Fast-ionic conductivity of Li^+ in $LiBH_4$

Tamio Ikeshoji,[1,*] Eiji Tsuchida,[2] Tetsuya Morishita,[2] Kazutaka Ikeda,[3] Motoaki Matsuo,[4]
Yoshiyuki Kawazoe,[4] and Shin-ichi Orimo[4,†]

[1]*New Industry Creation Hatchery Center (NICHe), Tohoku University, 6-6-10 Aoba, Aramaki, Aoba-ku, Sendai 980-8579, Japan*
[2]*Nanosystem Research Institute, National Institute of Advanced Industrial Science and Technology (AIST), AIST Tsukuba Central 2, 1-1-1 Umezono, Tsukuba 305-8568, Japan*
[3]*Institute of Materials Structure Science, KEK, 1-1 Oho, Tsukuba 305-0801, Japan*
[4]*Institute for Materials Research, Tohoku University, 2-1-1 Katahira, Sendai 980-8577, Japan*

(Received 8 November 2010; revised manuscript received 15 January 2011; published 6 April 2011)

High Li^+ conductivity in the high-temperature (hexagonal) phase of $LiBH_4$ is revealed through a first-principles molecular dynamics simulation of 1200 atoms using periodic boundary conditions. The high ionic conductivity originates from the generation of a Li^+ metastable state located at an interstitial site surrounded by three Li^+ ions and three BH_4^- ions in the *a*-*b* plane. A defect is created by Li^+ ions hopping from their original sites to this interstitial site. The defect then diffuses through a path connecting the nearby Li sites separated in the *a* and *c* directions. Coupling of these movements is observed. The double splitting of the Li occupation in the original Li site plays an important role in the creation of the metastable state and migration through the connection path. The activation energy and diffusion coefficient are estimated, and are within one order of magnitude of experimentally retrieved values.

DOI: 10.1103/PhysRevB.83.144301 PACS number(s): 66.30.Dn, 71.15.Pd, 82.45.Gj

I. INTRODUCTION

Fast ionic conductivity on the order of 10^{-3} S cm^{-1} can be found in some solid electrolytes.[1–3] This ionic conductivity is on the same order as those of electrolyte solutions. Several mechanisms governing this fast ionic conductivity have been proposed. If ions could occupy various sites and form a molten sublattice, those ions would be in a high-ionic-conductivity state as observed in α-AgI, for instance. Another type of ion conduction operates through defects or interstitial atoms formed by the introduction of different valence ions. Intrinsic defect and interstitial atom formation generally gives only low ionic conductivity except in the case of some materials, such as Li_3N,[4] Li_2NH,[5] and Li_3PO_4,[6] in which an enhanced intrinsic conductivity can be observed.

Development of fast ionic conductors is currently focused on Li^+, H^+, and O^{2-} for use in batteries or fuel cells. Solid-state Li ion conductors could be applied to solid lithium secondary batteries, which are safer and easier to handle than batteries using electrolytes in organic solvents. In addition to the solid lithium ion conductors mentioned above, the following types have been proposed: solid solutions and glasses with two or three components such as LiO_2-Zn0-GeO_2 and Li_2S-P_2S_5,[1,7,8] and others such as Li_2SO_4 and $Li_4BN_3H_{10}$.[1,9,10] However, a new type of solid Li ion conductor that has high Li ion conductivity and high chemical stability in anode and cathode regions is required for further development of lithium secondary batteries. To develop an electrolyte with higher ion conductivity, it is necessary to investigate the mechanism of ion conduction.

Recently, $LiBH_4$ was found to be superionic at $T > 390$ K (Li^+ conductivity $\sigma = 5 \times 10^{-3}$ S cm^{-1} at 423 K),[11] where it changes from an orthorhombic to a hexagonal structure. $LiBH_4$ is chemically stable with Li metal, and electrochemically reversible electron transfer takes place between Li^+ and Li metal.[11] Although $LiBH_4$ is a strong reducing agent, it has a large electrochemical window.[12] Some families of materials, such as those that can substitute BH_4^- for Br^- or I^-, also showed the same high ionic conductivity with lower phase-transition temperatures.[13,14] The partial substitution of Li by the divalent anion, Mg, did not increase the ionic conductivity.[15] No molten sublattice was reported in x-ray diffraction measurements. Although intrinsic ion conduction is expected from these results, a different mechanism of enhancement for the ionic conductivity should be found. A key to finding the mechanism may be the fact that the high temperature (hexagonal) phase of $LiBH_4$ has a doubly split Li atom occupation at 410 K, which we showed using first-principles molecular dynamics (FPMD) simulations with $54LiBH_4$ (384 atoms) under periodic boundary conditions.[16] In this paper, from a FPMD simulation of $200LiBH_4$ (1200 atoms) at 560 K with no additional impurities, we found that Li^+ diffuses in the crystal by generating a Li-atom metastable state located at the interstitial site and a connection path between the two original Li sites.

II. CALCULATIONS

Hexagonal-phase $LiBH_4$ was modeled using 1200 atoms ($200LiBH_4$) in a $21.62 \times 14.98 \times 35.23$ $Å^3$ supercell, which corresponds to $5 \times 4 \times 5$ lattice units ($2LiBH_4$). This is shown in Figs. 1(a) and 1(b). The lattice sizes are those obtained by x-ray diffraction experiments at 560 K.[17] In the FPMD simulations, atomic forces were calculated using density functional theory[18,19] with norm-conserving pseudopotentials.[20] The Kohn-Sham orbitals were expanded using the finite element basis functions[21] with an average cutoff energy of 64 Ry. These orbitals were quenched to the Born-Oppenheimer surface at each molecular dynamics (MD) step. The equations of motion for the atoms were integrated using the velocity-Verlet method at a time step of 40 a.u. (0.97 fs), and 15 000 steps were sampled after 10 000 equilibration steps. The temperature was kept constant at

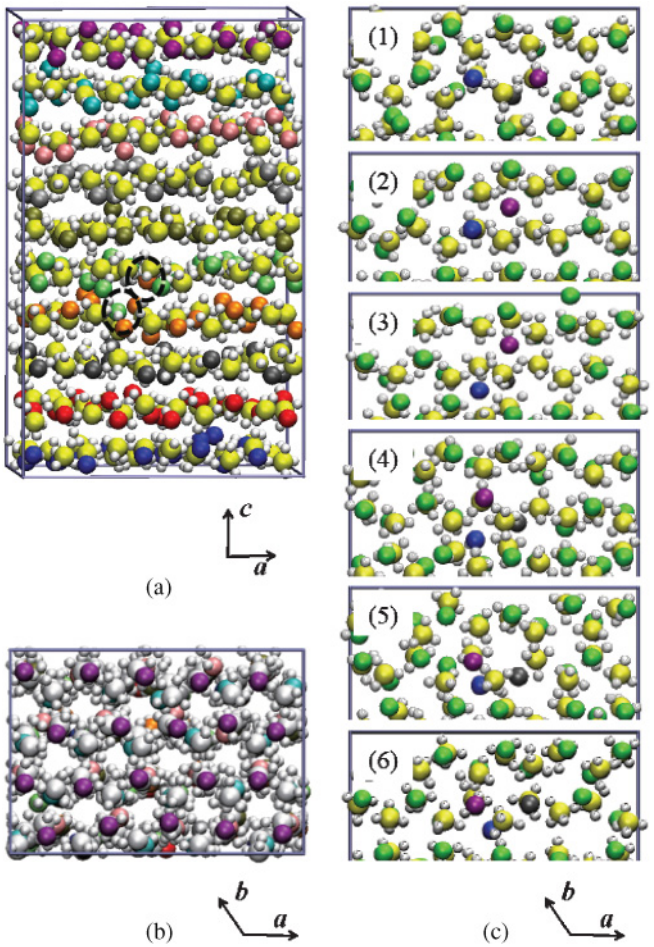

FIG. 1. (Color online) Snapshots of the 1200-atom first-principles molecular dynamics simulation of $LiBH_4$. (a) Side view of a lattice cell along the c axis. (b) Top view of the a-b plane. (c) Li-hopping events operated by three Li atoms. In (a) and (b), different colors show Li atoms originally located in the different layers, and the dashed circle shows Li atoms that have moved in the c direction. In (c) two layers are chosen. (1; 0 ps) Three Li atoms of different colors are at the original site. (2; 0.9 ps) A Li atom moves to the empty hole. (3; 1.5 ps) Another Li atom moves to a different empty hole. (4; 1.7 ps) The first Li atom moves to the vacancy made in (3). (5; 2.1 ps) The third Li atom moves to the vacancy made in (2). (6; 2.4 ps) The second atom moves to the vacancy made in (5). Yellow ball, B; white ball, H; green and other balls, Li.

560 K.[22] To keep the computational costs manageable, two additional techniques were used.

First, in the electronic-structure calculation, each orbital was allowed to take nonzero values only in a given region of space,[23,24] which enabled us to find the ground state with a linearly scaling computational cost.[25,26] We allocated one localized orbital of radius 10 a.u. (5.3 Å) to each lithium atom, and four localized orbitals of radius 14 a.u. (7.4 Å) to each boron atom. This was achieved by taking into account the properties of the maximally localized Wannier functions[27] in this system.[16] The use of this linearly scaling method reduced the execution time per MD step by a factor of 2.5 without sacrificing accuracy. Second, to make the MD calculations more efficient, we took advantage of the fact that the ensemble averages, such as radial distribution functions and free energies, do not depend on the atomic masses.[28] In this case, the atomic masses m were rescaled to $m_H = 1.236\,44$, $m_{Li} = 0.284\,44$, and $m_B = 4.444\,44$ following the treatment in Ref. 28. These were chosen to minimize the mismatch between the slow motion of the lithium atoms ($\leqslant 500\ cm^{-1}$) and the fast B−H stretch motion ($2400\ cm^{-1}$) of the original system.[16] We were able to achieve a fourfold to fivefold enhancement of the phase-space sampling of the lithium atoms. Further details of the simulations are given in Ref. 16.

III. RESULTS AND DISCUSSION

A. Li atom distribution (metastable site and connection region)

The space group $P6_3mc$ in a hexagonal structure is proposed for the high temperature phase of $LiBH_4$ from the x-ray- and neutron-diffraction measurements.[17,29–31] Its structure, however, shows instability (imaginary-frequency mode) during first-principles calculations at 0 K.[32–35] Structure optimization results in Li-atom movement along the $+c$ and $-c$ directions in the hexagonal lattice. FPMD simulations have shown double splitting and diffuse occupation of Li-atom states in this system at 410 K while maintaining the proposed lattice structure.[16] The x-ray diffraction pattern calculated from the FPMD trajectory was consistent with that observed experimentally, showing space group $P6_3mc$. Diffuse occupation was also confirmed from the Rietveld analysis for the measured x-ray diffraction pattern.[16] Li diffusion was not observed within the 15-ps simulation time with 384 atoms. From the NMR measurements, the jump frequency of the Li atoms was obtained; the Li^+ ion jumps every 12 ns at 400 K and every 0.47 ns at 500 K.[11] Therefore, if we increase the number of Li atoms and the temperature, Li hopping can be observed within the FPMD simulation time. Several Li hopping events were detected for $LiBH_4$ and $LiBD_4$ at 560 K in the 15-ps FPMD simulations when the system size was increased to 1200 atoms ($200LiBH_4$). The mixing of the Li atoms of the different layers was observed and is shown in Fig. 1(a). A Li-hopping event is shown in Fig. 1(c). Although we could determine all atom trajectories from the MD calculation, these trajectories in the absolute coordinates did not yield clear interpretations of the Li atom movement. We analyzed the trajectories after converting the atom positions to the coordinates system relative to the B atoms, which is explained below. In these simulations, no defects are introduced artificially.

The hexagonal structure made by three B and three Li atoms are shown from a top view in Fig. 1(b) [and also Fig. 3(a)]. Each layer in the a-b plane stacks a Li atom on a B atom and vice versa. The center of the hexagon is empty. There are two types of triangles made by B atoms. One has an empty hole at the center, and another has a Li atom. Moving Li atoms were identified by position relative to the three vectors from the empty hole toward the Li center, the B atom in the same plane, and another empty hole at the upper or lower side. Data from all equivalent positions were summed. Li-atom density ρ_{Li} is converted to free energy E, and $E = -RT[\log(\rho_{Li}/\rho^0_{Li})]$. The zero point is at Li density equal to ρ^0_{Li}. The maximum

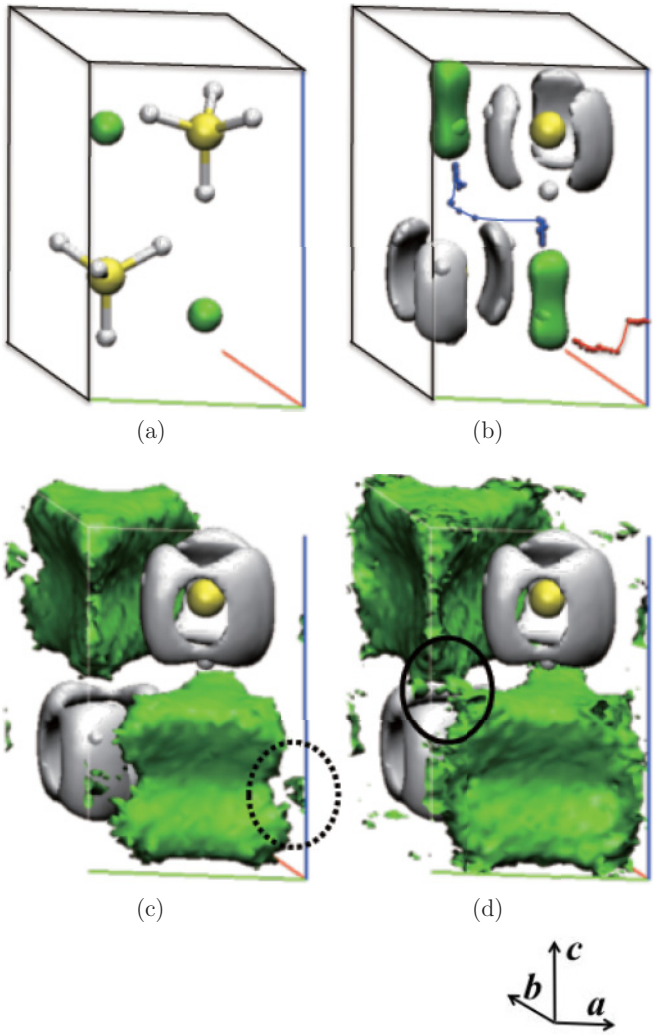

FIG. 2. (Color online) Free energy (E) surfaces of the Li atom at $E = 0.05$ eV (a), $E = 0.30$ eV (b), $E = 0.31$ eV (c), $E = 0.32$ eV (d). Green region, Li; yellow ball, B; white region, H; red line, energy minimum path to a metastable interstitial site from a Li site; blue line, energy minimum path to a connection region from a Li site.

density of Li (in the ground state) was used as the value, ρ^0_{Li}. The system is assumed to be in equilibrium. Figure 2 shows the isosurfaces of the Li-atom energy at various values, in which mass-scaled FPMD calculation results were used. Although B and H atoms are shown by balls at positions obtained through crystallography in Fig. 2(a), the BH_4 groups are in nearly free rotation. As can be seen in Fig. 2(b), Li atoms are distributed in a double splitting, resulting in a dumbbell-shape distribution.[16] When the drawing energy of the isosurface becomes high, a Li metastable state appears as indicated by the dashed circle in Fig. 2(c). It is located at the empty center of the hexagon made by three Li and three B atoms. It is in the plane of the middle of the doubly split Li sites. When we look at the high-energy surface, connections between Li-atom regions are found as indicated by a dashed circle in Fig. 2(d). The upper side of a Li region and the lower side of another Li region are connected by a narrow path.

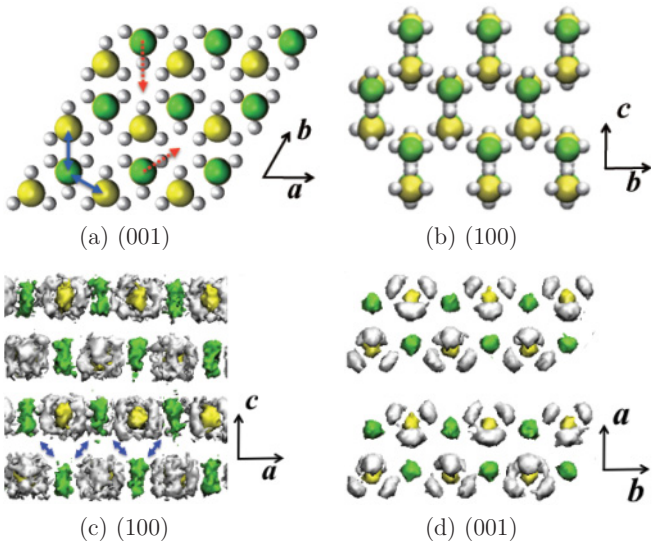

FIG. 3. (Color online) High temperature [(a), (c); hexagonal] and low temperature [(b), (d); orthorhombic] phase structures of $LiBH_4$. The red arrows indicate Li movement to the empty site (metastable site). The blue arrows indicate Li paths. Green region, Li; yellow region, B; white region, H.

B. Diffusion path

The hexagonal structure [Fig. 3(a)] can be found even in the low temperature (orthorhombic) phase of $LiBH_4$. This can be seen in Fig. 3(b), when the (100) plane is viewed.[31] A side view [Fig. 3(d)] of this phase is also similar to that of the high temperature phase [Fig. 3(c)], but the atoms are only vibrating around the local minima of the orthorhombic structure, which is indicated by the atom density in Fig. 3(d). BH_4 groups are not freely rotating, but complete rotation is sometimes observed.[36] When the temperature is increased, $LiBH_4$ has a phase transition to the higher symmetry hexagonal phase, and the Li occupation undergoes a double splitting.[16] Because of the splitting, there is a metastable interstitial site at the center of the empty hexagon in the a-b plane [Fig. 3(a) and Fig. 2(c)]. At the same time, it is possible to have a path connecting the Li regions that are closest together in the a-c direction. This is shown in Fig. 3(c) and Fig. 2(d).

Li atoms may diffuse in the following way. First, a Li atom moves to a metastable interstitial site by thermal excitation, leaving a vacancy. A probable path from the Li ground state to the metastable state is shown by the red line in Fig. 2(b). Energy changes along this path are shown in Fig. 4(a). The metastable-state energy is 0.29 eV and the barrier surrounding it is at 0.30 eV. Then, another Li atom moves to this vacancy through the connection region [Fig. 2(d)]. Li atoms can move in the a and c directions through the connection regions. This is indicated by a blue line in Fig. 2(b). Energy change along this path is shown in Fig. 4(b); the barrier height is 0.31 eV. If the Li atom in the metastable interstitial site returns to the defect, diffusion propagation is terminated. This is explained in Fig. 1(c), where several Li atoms are coupled in the diffusion process. The barrier heights are related to the measured activation energy, 0.51 eV.[11] The lower estimates may come from the fact that the Li-atom density in this MD-simulation analysis includes those atoms which do not contribute to the

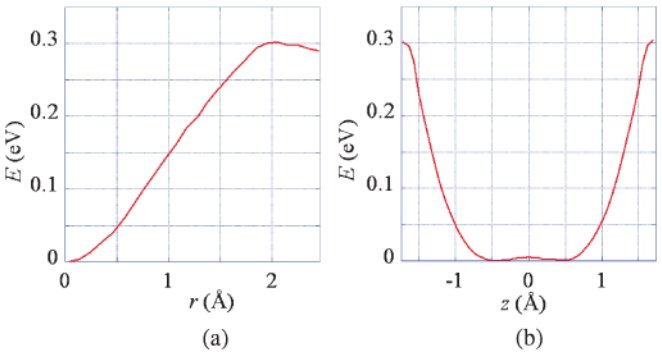

FIG. 4. (Color online) Energy profiles from the Li center to the metastable state (a) in the r direction on the a-b plane, and to the connection regions (b) in the z direction.

diffusion constructively. Therefore, some Li atoms move to the connection region, but they returned to the original sites shortly thereafter.

This kind of intrinsic defect-formation (Frenckel-pair formation) scheme is generally found in low-ionic-conductivity electrolytes. It is also found in fast ionic conductors like Li_3N,[4] Li_2NH,[5] and Li_3PO_4.[6] In these materials the interstitialcy is the main component of the high ionic conductivity. In the case of $LiBH_4$, interstitialcy contributes in another way: a metastable state induces a vacancy that disallows direct hopping from one metastable to another. Direct hopping from a Li site to a nearby Li site is possible. The doubly split occupation of the original Li site plays an important role, and the Li atom at the interstitial site is metastable.

Ionic conductivity σ is related to the diffusion coefficient D of the ion by $\sigma = D(Ze)^2\rho_{\mathrm{Li}}/(RT)$, where Z is charge number of the ion and e is the unit charge. Because only a few hopping events were observed within 15 ps in the 1200-atom simulations of $LiBH_4$ and $LiBD_4$, the evaluation of the diffusion coefficient includes a large margin of error. The estimated values of the mean-squared displacements of the Li atoms obtained through FPMD using unscaled masses are 0.4–1 $cm^2\ s^{-1}$. They correspond to values of 0.1–0.3 S cm^{-1} at 560 K, if we use a Li concentration in the simulated system of ρ_{Li}. They are in good agreement with the experimental value, 0.14 S cm^{-1}, at 560 K.[11]

IV. CONCLUSIONS

The FPMD simulations showed that the high ionic conductivity of $LiBH_4$ originates from the atom occupation splitting in the c direction that results in a dumbbell-like density profile. This generates a metastable interstitial site centered among the three Li atoms and three BH_4 groups in the a-b plane and the connection paths between two closest Li sites in the a-c direction. Li atoms can diffuse through the connection paths in the three directions. Our finding that the high ionic conductivity originates from the doubly split occupation (dumbbell type) of the Li atoms will provide a new interstitialcy-based mechanism for fast-ionic conductivity.

ACKNOWLEDGMENTS

We thank J. Kawamura for helpful discussion and suggestions. The numerical calculations were performed on PC clusters at AIST and the Research Institute for Information Technology, Kyushu University. This work was supported in part by KAKENHI (Grants No. 22760529 and No. 21246100), Funding Program for Next Generation World-Leading Researchers (GR008), and the Inter-university Cooperative Research Program of the Institute for Materials Research, Tohoku University. 3D images were generated using VMD.[37]

*ikeshoji@niche.tohoku.ac.jp
†orimo@imr.tohoku.ac.jp

[1] S. Hull, Rep. Prog. Phys. **67**, 1233 (2004).
[2] A. K. Ivanov-Shitz, Crystallogr. Rep. **52**, 302 (2007).
[3] P. P. Kumar and S. Yashonath, J. Chem. Sci. **118**, 135 (2006).
[4] J. Sarnthein, K. Schwarz, and P. E. Blochl, Phys. Rev. B **53**, 9084 (1996).
[5] C. M. Araújo, A. Blomqvist, R. H. Scheicher, P. Chen, and R. Ahuja, Phys. Rev. B **79**, 172101 (2009).
[6] Y. A. Du and N. A. W. Holzwarth, Phys. Rev. B **76**, 174302 (2007).
[7] P. G. Bruce and A. R. West, J. Solid Chem. **4**, 354 (1982).
[8] M. Murayama, N. Sonoyama, A. Yamada, and R. Kanno, Solid State Ionics **170**, 173 (2004).
[9] M. Ferrario, M. Klein, and I. R. McDonald, Molec. Phys. **86**, 923 (1995).
[10] D. E. Farrell, D. Shin, and C. Wolverton, Phys. Rev. B **80**, 224201 (2009).
[11] M. Matsuo, Y. Nakamori, S. Orimo, H. Maekawa, and H. Takamura, Appl. Phys. Lett. **91**, 224103 (2007).
[12] M. Matsuo and S.-i. Orimo, Adv. Energy Mater. **1**, 161 (2011).
[13] M. Matsuo, H. Takamura, H. Maekawa, H.-W. Li, and S. Orimo, Appl. Phys. Lett. **94**, 084103 (2009).
[14] H. Maekawa, M. Matsuo, H. Takamura, M. Ando, Y. Noda, T. Karahashi, and S. Orimo, J. Am. Chem. Soc. **131**, 894 (2009).
[15] M. Matsuo and S. Orimo (unpublished results).
[16] T. Ikeshoji, E. Tsuchida, K. Ikeda, M. Matsuo, H.-W. Li, Y. Kawazoe, and S. Orimo, Appl. Phys. Lett. **95**, 221901 (2009).
[17] Y. Filinchuk, D. Chernyshov, and R. Cerny, J. Phys. Chem. C **112**, 10579 (2008).
[18] R. M. Martin, *Electronic Structure: Basic Theory and Practical Methods* (Cambridge University Press, New York, 2004).
[19] J. P. Perdew, K. Burke, and M. Ernzerhof, Phys. Rev. Lett. **77**, 3865 (1996).
[20] S. Goedecker, M. Teter, and J. Hutter, Phys. Rev. B **54**, 1703 (1996).
[21] E. Tsuchida and M. Tsukada, J. Phys. Soc. Jpn. **67**, 3844 (1998).
[22] H. J. C. Berendsen, J. P. M. Postma, W. F. van Gunsteren, A. DiNola, and J. R. Haak, J. Chem. Phys. **81**, 3684 (1984).
[23] G. Galli and M. Parrinello, Phys. Rev. Lett. **69**, 3547 (1992).
[24] E. Tsuchida, J. Phys. Soc. Jpn. **76**, 034708 (2007); J. Phys. Condens. Matter **20**, 294212 (2008).
[25] T. Ozaki, Phys. Rev. B **74**, 245101 (2006).
[26] D. R. Bowler and T. Miyazaki, J. Phys. Condens. Matter **22**, 074207 (2010).
[27] N. Marzari and D. Vanderbilt, Phys. Rev. B **56**, 12847 (1997).

[28]E. Tsuchida, J. Chem. Phys. **134**, 044112 (2011).
[29]F. Buchter, Z. Lodziana, Ph. Mauron, A. Remhof, O. Friedrichs, A. Borgschulte, A. Zuttel, D. Sheptyakov, Th. Strassle, and A. J. Ramirez-Cuesta, Phys. Rev. B **78**, 094302 (2008).
[30]M. R. Hartman, J. J. Rush, T. J. Udovic, R. C. Bowman Jr., and S-J. Hwang, J. Solid State Chem. **180**, 1298 (2007).
[31]G. Soulie, J-Ph. Renaudin, R. Cerny, and K. Yvon, J. Alloys. Compd. **346**, 200 (2002).
[32]Z. Lodziana and T. Vegge, Phys. Rev. Lett. **93**, 145501 (2004); *ibid*. **97**, 119602 (2006).
[33]N. A. Zarkevich and D. D. Johnson, Phys. Rev. Lett. **97**, 119601 (2006); **100**, 040602 (2008).
[34]T. J. Frankcombe and G.-J. Kroes, Phys. Rev. B **73**, 174302 (2006).
[35]K. Miwa, N. Ohba, S.-i. Towata, Y. Nakamori, and S.-i. Orimo, Phys. Rev. B **69**, 245120 (2004).
[36]A. Remhof, Z. Lodziana, P. Martelli, O. Friedrichs, A. Zuttel, A. V. Skripov, J. P. Embs, and T. Strassle, Phys. Rev. B, **81**, 214304 (2010).
[37]W. Humphrey, A. Dalke, and K. Schulten, J. Molec. Graphics **14**, 33 (1996); [http://www.ks.uiuc.edu/Research/vmd/].